Research Article

Mathematical Methods in the Applied Sciences

Received 20 February 2013

Published online in Wiley Online Library

(wileyonlinelibrary.com) DOI: 10.1002/mma.2864
MOS subject classification: 92

Mathematical modeling for multisite phosphorylation with scaffold binding in cell signaling

Kanadpriya Basu[a,b] and Xinfeng Liu[a*†]

Communicated by Q. Wang

The mating decision in budding yeast is a switch-like or bistability response that allows cells to filter out weak pheromone signals or avoid improper mating when a mate is sufficiently close. However, the molecular mechanisms that control the bistability decision are not yet fully understood. In many cases, scaffold proteins are thought to play a key role during this process. A workable definition of a scaffold is a protein that dynamically binds to two or more consecutively acting components of a signaling cascade, such as protein kinase and that kinase's substrate. Here, we show that bistability mechanism can arise from multisite phosphorylation system with scaffold binding when phosphorylation and dephosphorylation occur at different locations. This scaffold binding in a multisite phosphorylation system can robustly result in multiple steady states. By developing generic mathematical models, we argue that the scaffold protein plays an important role in creating bistability, and by treating parameters symbolically, we also thereby reduce the complexity of calculating steady states from simulating differential equations to finding the roots of polynomials, of which the degree depends on the number of phosphorylation sites *N*. Copyright © 2013 John Wiley & Sons, Ltd.

Keywords: multisite phosphorylation; MAP kinase cascades; bistability; scaffold proteins

1. Introduction

When a hormone or growth factor binds to a cell-surface receptor, a cascade of proteins inside the cell relays the signal to specific intracellular targets. Proteins referred to as 'scaffolds' or 'anchoring proteins' are thought to play many important roles during this process [1–3]. A workable definition of a scaffold is a protein that dynamically binds to two or more consecutively acting components of a signaling cascade, such as protein kinase and that kinase's substrate. In doing so, scaffolds are thought to increase the rate of signal transmission between those components (e.g., by increasing the rate at which the kinase phosphorylates its substrate) [4–6]. Scaffold proteins are also thought to increase the specificity of signaling, and several mechanisms by which they may accomplish this have been proposed [7, 8]. In the budding yeast, well-known examples of scaffold protein include yeast Ste5, which binds to all kinases in a particular mitogen-activated protein kinase (MAP kinase) cascade [1–3, 9–12] (see Figure 1(a) for the illustration), whereas the MAP kinase cascades that are evolutionally conserved from budding yeast to mammals play a pivotal role in many aspects of cellular functions.

By adding a phosphate group (PO_3) to one or more amino acid residues, the phosphorylation (phosphate addition) or dephosphorylation (phosphate removal) of a protein can alter its behavior in almost every conceivable way [13–15]. The three-protein motif consisting of a kinase, the substrate it phosphorylates, and the phosphatase that undoes the phosphorylation can be viewed as a fundamental module in cellular regulation [16]. The functions of phosphorylation or dephosphorylation of a protein include regulation of its intrinsic biological activity, subcellular activity, half life, and docking with other proteins. In contrast to phosphorylation with a single residue, multisite phosphorylation can enable several such effects to operate in the same protein and thus can determine the extent and duration of a response during signal integration. Furthermore, multisite phosphorylation increases considerately the possibilities for regulating protein functions. For instance, a protein with N phosphorylation sites can have 2^N phosphorylation states, and each such state may have its own functional characteristics. Examples of proteins that are found to harbor multiple phosphorylation sites include membrane receptors [17, 18], ion channels [19], protein kinases (e.g., MAP kinases [20, 21], and Src family kinases [22]).

[a] *Department of Mathematics, University of South Carolina , Columbia, SC 29208, USA*
[b] *Department of Mathematics, University of North Texas, Denton, TX 76203, USA*
**Correspondence to: Xinfeng Liu, Department of Mathematics, University of South Carolina, Columbia, SC 29208, USA.*
[†] *E-mail: xfliu@math.sc.edu*

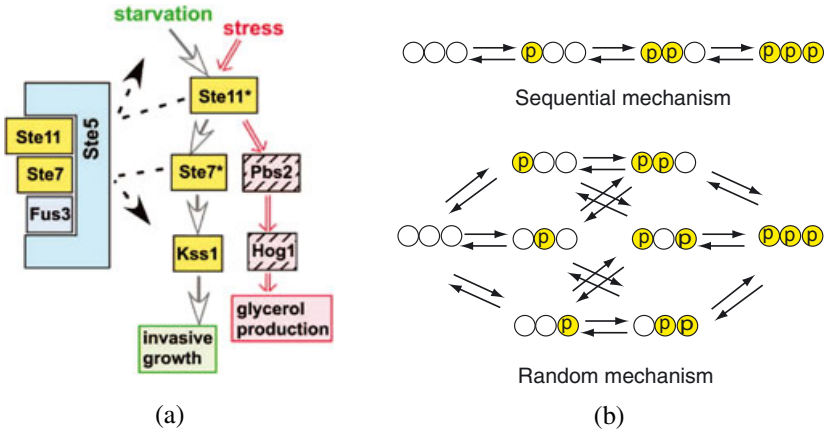

Figure 1. (a) Schematic diagram of MAP kinase cascades [23]. (b) Order of phosphosite processing. Phosphorylation sites may follow a strict sequential order (top) or a completely random order (bottom) [24].

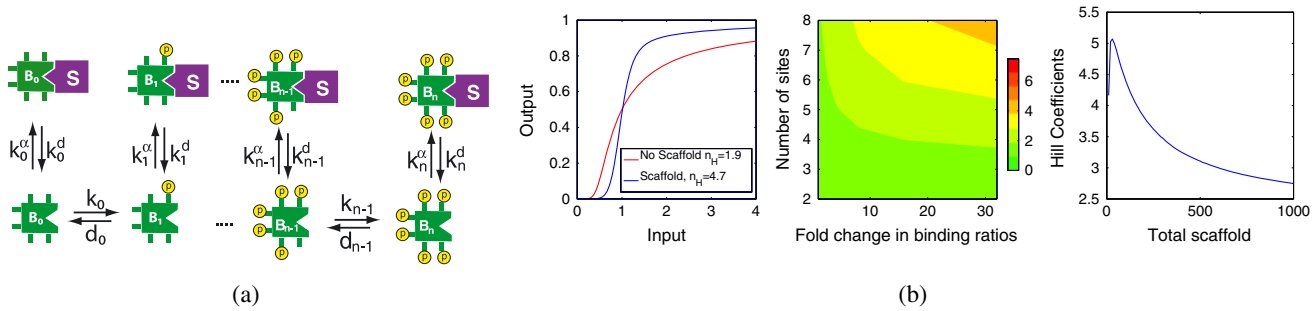

Figure 2. (a) A schematic diagram depicting substrate sequestration in a multisite phosphorylation system with the kinase away from the scaffolds; (b) compared with a system without scaffold, substrate sequestration in a multisite phosphorylation system is able to foster a better switch (left). Contour plots of solutions by Hill coefficients show that the switch-like responses rely heavily on scaffold binding ratios with successive phosphorylations (middle), and the simulations also indicate that there exists an optimum total scaffold for a best switch (right).

Ultrasensitivity/switch-like responses and bistability, which can be used in signal transduction to filter out noises while amplifying weak inputs, are recurring themes in cell signaling [10, 25–29]. It has often been presumed that a multisite phosphorylation mechanism intends to increase the level of switch-like responses. Compared with a single-site target, the possibilities for multisite phosphorylation in the regulation of protein–protein regulation interactions and the phosphorylation sequence are increased dramatically, thus providing additional mechanisms for the generation of ultrasensitivity and/or bistability. However, as shown in [30], this presumption only holds true if the ratios of phosphorylation and dephosphorylation for the first and last states are significantly stronger than the intermediate phosphorylation states (i.e., those states other than completely unphosphorylated and completely phosphorylated) [30, 31].

Hence, multisite phosphorylation, by itself, is not sufficient to generate a switch-like response. In [31], it is revealed that the combination of multisite phosphorylation and membrane binding could produce a switch-like dissociation of Ste5 from the membrane. Recent studies [32] have demonstrated that the maximal number of possible steady states increases with the number of phosphorylation sites. In [33], by reducing the complexity of calculating steady states by solving two algebraic equations when treating parameters symbolically, it was shown that a multisite phosphorylation system exhibits distinct stable phosphoform distribution at steady states. However, none of the aforementioned findings include scaffold binding for a multisite phosphorylation system, which is a key feature in many biological systems [34–40]. More recently in [10], it is shown that the switching mechanism arises from competition between the MAP kinase Fus3 and a phosphatase Ptc1 for control of the phosphorylation state of four sites on the scaffold protein Ste5.

Previously in [41], we have studied the effects of scaffold binding with multisite phosphorylation on the switch-like responses and mainly focused on exploring the scenarios when both phosphorylation and dephosphorylation of the substrate take place either on the scaffold or away from the scaffold (Figure 2(a)). By modulating both stronger and weaker scaffold binding with successive phosphorylations, as well as the elaborate combinations of these two strategies, our findings suggest that scaffold binding can robustly enhance the multisite phosphorylation system resulting in a good switch and threshold (also see Figure 2(b)).

In this paper, by developing generic mathematical models together with computational exploration with random sampling of parameters, we will be focusing on studying the effects of scaffold binding in a multisite phosphorylation system on the generation of

bistability when phosphorylation and dephosphorylation take place at different locations. First, we consider the system when the kinase is co-localized on the scaffold while dephosphorylation is away from the scaffold. Second, we study another system when dephosphorylation occurs on the scaffold while phosphorylation is off the scaffold. The numerical simulations integrated with mathematical analysis by solving the steady-state solutions of a system of differential equations reveal that both the aforementioned systems robustly lead to bistability with a wide range of parameters. Finally, a brief conclusion is drawn.

2. Results

Mathematical models developed over the recent years have shed light on the variety of molecular mechanisms with multisite phosphorylations [24, 30, 32, 33]. For the presence of enzyme–substrate and phosphatase–substrate complexes, where the kinase and phosphatase are saturated, the system takes the following form:

$$B_i + A \rightleftharpoons AB_i \rightarrow B_{i+1} + A; \quad B_{i+1} + F \rightleftharpoons FB_{i+1} \rightarrow B_i + F. \tag{1}$$

where $B_{i,i+1}$, A, and F represent phosphoform with i or $i+1$ sites phosphorylated, enzyme, and phosphatase, respectively. The results for such system with scaffold binding in a multisite phosphorylation system have been reported in a separate publication [42]. For this paper, we are particularly interested in cases where the kinase and phosphatase are not saturated. Thus, we ignore enzyme–substrate and phosphatase–substrate complexes and use the following scheme:

$$B_i + A \rightarrow B_{i+1} + A; \quad B_{i+1} + F \rightarrow B_i + F, \tag{2}$$

By removing the possibility of enzyme sequestration effects, such cases are initially the motivation for proposing multisite phosphorylation as an alternative means besides Michaelis–Menton kinetics to achieve ultrasensitivity [24, 30, 43–46]. In this paper, we also make an assumption that phosphorylation sites follow a strictly sequential phosphorylation mechanism (Figure 1(b), top), in which there are only $N+1$ phosphorylation states instead of 2^N. This simplification also provides analytical tractability and thus allows for finding the solution in the roots of polynomials and dramatically reduces the computational complexity.

As discussed in [41] , if the phosphorylation and dephosphorylation only take place away from the scaffold, there exists only one steady state for the system. Similarly, the same conclusion holds if phosphorylation and dephosphorylation only occur for scaffold-bound substrates. Thus, to allow for bistability, phosphorylation and dephosphorylation must take place on different locations; that is, if one happens on the scaffold, the other one must take place away from the scaffold, and vice versa. (Figure 3(a, b)). In the following two sections, we will separately consider these two cases one by one.

2.1. *Kinase co-localized on the scaffold*

In cell signaling, scaffold proteins act as organizing platforms that bind to both a kinase and its substrate and thereby facilitate the phosphorylation of the substrate by the kinase. A prime example is the yeast MAP kinase Fus3 (here playing the role of substrate), which can only be phosphorylated by its activator Ste7 if both Fus3 and Ste7 are bound to the Ste5 scaffold protein. Therefore, a reasonable way to model a situation like this is to assume that the substrate can only be phosphorylated when bound to the scaffold protein. For this case when the kinase is co-localized on the scaffold (Figure 3(a)), the system of equations with the mechanism of mass action takes the following form:

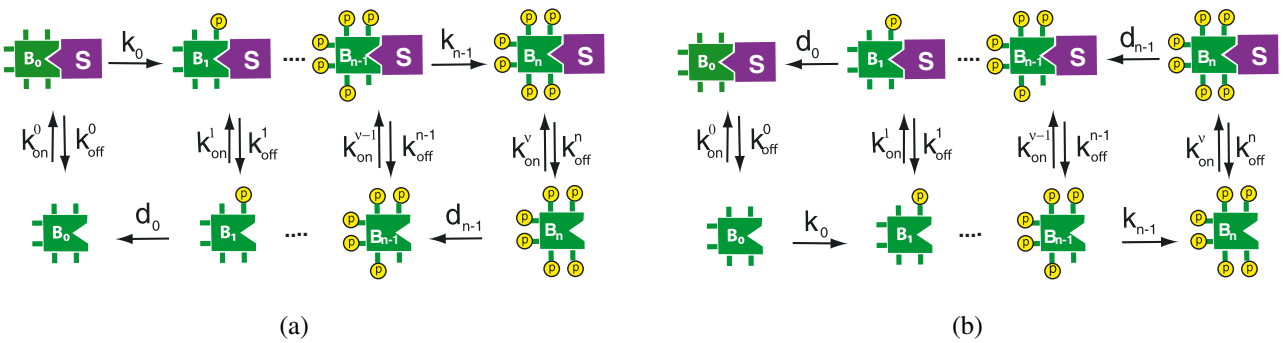

Figure 3. (a) Schematic diagram of the system with the kinase co-localized on the scaffold while dephosphorylation occurs away from the scaffold; (b) diagram of the system when dephosphorylation takes place on the scaffold while the kinase is away from the scaffold.

$$\begin{cases} [B_0]' = d_0[B_1] - k^0_{\text{on}}[B_0][S] + k^0_{\text{off}}[B_0S], \\ [B_1]' = -d_0[B_1] + d_1[B_2] - k^1_{\text{on}}[B_1][S] + k^1_{\text{off}}[B_1S], \\ \vdots \\ [B_n]' = -d_{n-1}[B_n] - k^n_{\text{on}}[B_n][S] + k^n_{\text{off}}[B_nS], \\ [B_0S]' = -k_0[B_0S][A] + k^0_{\text{on}}[B_0][S] - k^0_{\text{off}}[B_0S], \\ [B_1S]' = k_0[B_0S][A] - k_1[B_1S][A] + k^1_{\text{on}}[B_1][S] - k^1_{\text{off}}[B_1S], \\ \vdots \\ [B_{n-1}S]' = k_{n-2}[B_{n-2}S][A] - k_{n-1}[B_{n-1}S][A] + k^{n-1}_{\text{on}}[B_{n-1}][S] - k^{n-1}_{\text{off}}[B_{n-1}S], \\ [B_nS]' = k_{n-1}[B_{n-1}S][A] + k^n_{\text{on}}[B_n][S] - k^n_{\text{off}}[B_nS], \\ [S]' = k^0_{\text{off}}[B_0S] - k^0_{\text{on}}[B_0][S] + \cdots + k^n_{\text{off}}[B_nS] - k^n_{\text{on}}[B_n][S], \end{cases} \tag{3}$$

where B_i, A, S, and B_iS represent phosphoform with i sites phosphorylated, enzyme, free scaffold, and scaffold binding complex, respectively, and [ ] denotes the concentration for each protein species, whereas [ ]′ stands for time derivatives. The parameter k_i is for the reaction rate with enzyme A for the ith phosphorylated substrate; the parameter d_i qualifies the rate of dephosphorylation from the $(i+1)$th phosphorylated form to the ith phosphorylated substrate; and k^i_{on} and k^i_{off} represent binding and dissociate rates of the substrate with scaffolds, respectively.

Here, we are interested in the steady states for the aforementioned system; that is, let the right-hand side of the aforementioned system equal to zero. Through some algebraic calculations, we observe that

$$\begin{aligned} [B_iS] &= \sum_{j=1}^{i+1} a^{i+1}_j [B_0][S]^j, \quad i = 0, 2, \ldots, n \\ [B_i] &= \sum_{j=1}^{i} b^i_j [B_0][S]^j, \quad i = 1, \ldots, n \end{aligned} \tag{4}$$

where $a^1_1 = \dfrac{k^0_{\text{on}}}{k^0_{\text{off}} + k_0[A]}$, $b^1_1 = \dfrac{k_0[A]}{d_0} a^1_1$, and the values for all other a's and b's can be found from the following equations:

$$a^{i+1}_1 = \begin{cases} \dfrac{k_{i-1}[A]}{k^i_{\text{off}} + k_i[A]} a^i_1, & \text{if } i = 1, \ldots, n-1 \\ \dfrac{k_n[A]}{k^{n+1}_{\text{off}}} a^n_1, & \text{if } i = n \end{cases} \tag{5}$$

$$a^{i+1}_{i+1} = \begin{cases} \dfrac{k^i_{\text{on}}}{k^i_{\text{off}} + k_i[A]} b^i_i, & \text{if } i = 1, \ldots, n-1 \\ \dfrac{k^i_{\text{on}}}{k^i_{\text{off}}} b^i_i, & \text{if } i = n \end{cases} \tag{6}$$

$$a^{i+1}_j = \begin{cases} \dfrac{k_{n-1}[A]a^n_j + k^n_{\text{on}} b^n_{j-1}}{k^n_{\text{off}}}, & \text{if } \ i = n, j = 2, \ldots, n, \\ \dfrac{k_{i-1}[A]a^i_j + k^i_{\text{on}} b^i_{j-1}}{k^i_{\text{off}} + k_i[A]}, & \text{if } \ i < n, j = 2, \ldots, i \end{cases} \tag{7}$$

$$b^i_j = \begin{cases} \dfrac{d_{i-2}b^{i-1}_1 - k^{i-1}_{\text{off}} a^i_1}{d_{i-1}}, & \text{if } j = 1, i = 2, \ldots, n \\ \dfrac{k^{i-1}_{\text{on}} b^{i-1}_{i-1} - k^{i-1}_{\text{off}} a^i_i}{d_{i-1}}, & \text{if } j = i \\ \dfrac{d_{i-2}b^{i-1}_j + k^{i-1}_{\text{on}} b^{i-1}_{j-1} - k^{i-1}_{\text{off}} a^i_{j-1}}{d_{i-1}}, & \text{if } j = 2, \ldots, n, i = 3, \ldots, j-1 \end{cases} \tag{8}$$

In addition, the concentrations for total substrates (denoted by B_t) and scaffolds (denoted by S_t) are conserved, and finally, the solution for the steady state of the free scaffold can be calculated through the following polynomial:

$$\sum_{i=1}^{n+2} C_i[S]^i = 0, \tag{9}$$

where

$$C_i = \begin{cases} a_{n+1}^{n+1}, & \text{if } i = n+2 \\ \sum_{j=i-1}^{n}(b_{i-1}^{j} + a_{i-1}^{j}) + a_{i-1}^{n} + \\ \quad \left(\sum_{j=i}^{n+1} a_i^j\right)(B_t - S_t) + \left(\sum_{j=i}^{n} b_i^j\right)S_t, & \text{if } i = n+1, \ldots, 2 \\ 1 + \left(\sum_{j=1}^{n+1}\right)B_t - \left(\sum_{j=1}^{n} b_1^j + \sum_{j=1}^{n+1} a_1^j\right)S_t, & \text{if } i = 1 \\ -S_t, & \text{if } i = 0 \end{cases} \tag{10}$$

For a simple special case with $n = 1$, the solutions for the concentration of $[S]$ at steady states are the roots of a cubic polynomial:

$$\begin{aligned} &a_2^2[S]^3 + \{a_2^2(B_t - S_t) + (b_1^1 + a_1^1 + a_1^2)\}[S]^2 + \\ &\{1 + (a_1^1 + a_1^2)B_t - (b_1^1 + a_1^1 + a_1^2)S_t\}[S] - S_t = 0 \end{aligned} \tag{11}$$

Through our computational exploration with random sampling of parameters, the aforementioned cubic polynomials only admits one positive root, and no bistability has been observed for this case with $n = 1$.

For the case when $n = 2$, the solutions of scaffold concentration at steady states can be found from solving a polynomial of degree 4:

$$\begin{aligned} a_3^3[S]^4 + \{a_3^3(B_t - S_t) + (b_2^2 + a_2^2 + a_2^3)\}[S]^3 + \{(b_1^1 + b_1^2 + a_1^1 + a_1^2 + a_1^3) \\ + (a_2^2 + a_2^3)B_t - (b_2^2 + a_2^2 + a_2^3)S_t\}[S]^2 + \{1 + (a_1 + a_1^2 + a_1^3)B_t \\ - (b_1^1 + b_1^2 + a_1^1 + a_1^2 + a_1^3)S_t\}[S] - S_t = 0 \end{aligned} \tag{12}$$

The aforementioned system with $n = 2$ exhibits multistabilities from our computational exploration. Such large-scale computations have been performed by random parameter sampling technique using the existing function roots() in MATLAB. First, we have carried out two computational experiments. In one experiment, we fix the total amount of substrate, whereas we vary the total amount of scaffold. For the second experiment, we change the total substrate with a fixed amount of the total scaffold. For both cases, the bistability takes place only for a certain amount of scaffold (with the total substrate fixed) and substrate (with the total scaffold unchanged). Moreover, the system leads to bistability for a larger range of total substrate than that of the total scaffold. In addition, our computation also suggests that the bistability tends to occur when the total substrate exceeds the total scaffold (Figure 4). One possible explanation

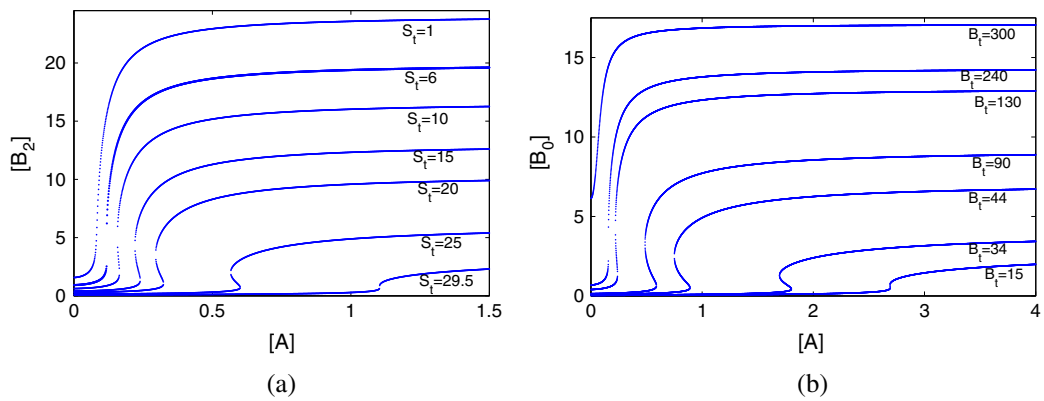

Figure 4. Simulation results with the kinase co-localized on the scaffold while dephosphorylation takes place away from scaffold for the case $n = 2$. For both simulations, the parameters are set up as follows: $k_{on}^0 = 2.85, k_{off}^0 = 1.43, k_{on}^1 = 7.6, k_{off}^1 = 7.42, k_{on}^2 = 0.09, k_{off}^2 = 7.23, k_0 = 0.96, d_0 = 3.75, k_1 = 6.47$, and $d_1 = 0.14$. (a) Bistability takes place for a variance of total scaffold with a fixed total amount of substrate $B_t = 45$; (b) bistability occurs for a variance of total substrate when the total scaffold is fixed to 20.

for this observation is that the bistability arises from the competition between different phosphorylation states when bound to free scaffold proteins, whereas either too many or too few scaffolds would obviously reduce the levels of such competition. Therefore, there should exist a certain range of scaffold proteins to allow for the bistability to happen.

Furthermore, for the system to allow for bistability, we also observed that the phosphorylation and dephosphorylation rates for the last phosphorylated form need to be at least $1/50$ smaller than those for all other states. All the aforementioned conclusions hold for the case $n = 3$. We also checked the system with the cases till $n = 8$ as well as two other randomly selected cases ($n = 10$ and $n = 16$), and a similar pattern for the system to generate bistability has been observed. These findings suggest that such pattern as observed for the case $n = 2$ can be expected for the general n as well.

2.2. *Dephosphorylation takes place on the scaffold*

For the system when dephosphorylation takes place on the scaffold while the kinase is off the scaffold, the mass action equations based on the reactions in Figure 3(b) take the following form:

$$\begin{cases} [B_0]' = -k_0[A][B_0] - k^0_{\text{on}}[B_0][S] + k^0_{\text{off}}[B_0S], \\ [B_1]' = k_0[A][B_0] - k_1[A][B_1] - k^1_{\text{on}}[B_1][S] + k^1_{\text{off}}[B_1S], \\ \vdots \\ [B_n]' = k_{n-1}[A][B_{n-1}] - k^n_{\text{on}}[B_n][S] + k^n_{\text{off}}[B_nS], \\ [B_0S]' = d_0[B_1S] + k^0_{\text{on}}[B_0][S] - k^0_{\text{off}}[B_0S], \\ [B_1S]' = -d_0[B_1S] + d_1[B_2S] + k^1_{\text{on}}[B_1][S] - k^1_{\text{off}}[B_1S], \\ \vdots \\ [B_{n-1}S]' = -d_{n-2}[B_{n-1}S] + d_{n-1}[B_nS] + k^{n-1}_{\text{on}}[B_{n-1}][S] - k^{n-1}_{\text{off}}[B_{n-1}S], \\ [B_nS]' = -d_{n-1}[B_nS] + k^n_{\text{on}}[B_n][S] - k^n_{\text{off}}[B_nS], \\ [S]' = k^0_{\text{off}}[B_0S] - k^0_{\text{on}}[B_0][S] + \cdots + k^n_{\text{off}}[B_nS] - k^n_{\text{on}}[B_n][S]. \end{cases} \tag{13}$$

Because the total amount of both the scaffold and substrate are conserved, once again we have the following two conservation equations:

$$B_t = \sum_{i=0}^{n}[B_i] + \sum_{i=0}^{n}[B_iS], \quad S_t = [S] + \sum_{i=0}^{n}[B_iS]. \tag{14}$$

For the steady states, the following equations hold for the steady-state solutions of $[B_i]$:

$$[B_i] = \begin{cases} \alpha^n_{-1}[B_{n-1}][S]^{-1}, & \text{if } i = n \\ \displaystyle\sum_{j=0}^{n-i-1} \alpha^i_j[B_{n-1}][S]^j, & \text{if } i = n-2, n-3, \ldots, 0 \end{cases} \tag{15}$$

where

$$\alpha^n_{-1} = \frac{(d_{n-1} + k^n_{\text{off}})}{k^n_{\text{on}}} \frac{k_{n-1}[A]}{d_{n-1}} = \frac{(d_{n-1} + k^n_{\text{off}})}{k^n_{\text{on}}} \beta^n_0 \tag{16}$$

and for $l = 1, \ldots, n-2$,

$$[B_l] = \sum_{j=0}^{n-l-1} \alpha^l_j[B_{n-1}][S]^j, \qquad i = 0, 1, \ldots, (n-2) \tag{17}$$

$$\alpha^l_j = \begin{cases} \dfrac{d_l}{k_l[A]}\beta^{l+1}_0, & \text{if } j = 0 \\ \dfrac{d_l}{k_l}\left(\dfrac{k_j}{k^j_{\text{on}}}\beta^{l+1}_o + \dfrac{k^j_{\text{on}}}{k_j[A]}\beta^{l+1}_{n-l-1}\right), & \text{if } j = 1, 2, \ldots, (n-l-2) \\ \dfrac{d_l}{k_l[A]}\beta^{l+1}_{n-l-1}, & \text{if } j = n-l-1 \end{cases} \tag{18}$$

Moreover,

$$[B_iS] = \sum_{j=0}^{n-i} \beta^i_j[B_{n-1}][S]^j, \qquad i = 0, 1, \ldots, n \tag{19}$$

The coefficients β_j^i are defined by

$$\beta_j^i = \begin{cases} \frac{k_0[A]}{k_{\text{off}}^0}\alpha_0^0, & \text{if } i=0, j=0 \\ \frac{k_{\text{on}}^0\alpha_{j-1}^0 + k_0[A]\alpha_j^0}{k_{\text{off}}^0}, & \text{if } i=0, j=1,\ldots,n-1 \\ \frac{k_{\text{on}}^0}{k_{\text{off}}^0}\alpha_{n-1}^0, & \text{if } i=0, j=n \\ \frac{k_i[A]}{d_{i-1}+k_{\text{off}}^i}\alpha_0^i, & \text{if } i=1,\ldots,n-2, j=0 \\ \frac{k_j[A]\alpha_i^j - k_{j-1}[A]\alpha_i^{j-1} + k_{\text{on}}^j\alpha_{i-1}^j}{k_{\text{off}}^j}, & \text{if } i=1,\ldots,n-2, j=1,\ldots,(n-i-1) \\ \frac{k_{\text{on}}^j}{d_{i-1}+k_{\text{off}}^i}\alpha_{n-i}^i, & \text{if } i=1,\ldots,n-2, j=n-i \\ \frac{k_{n-1}[A]}{d_{n-1}}, & \text{if } i=n, j=0 \\ \frac{k_{n-1}[A]}{d_{n-2}+k_{\text{off}}^{n-1}}, & \text{if } i=n-1, j=0 \\ \frac{k_{\text{on}}^{n-1}}{d_{n-2}+k_{\text{off}}^{n-1}}, & \text{if } i=n-1, j=1 \end{cases} \tag{20}$$

The steady-state solution of $[S]$ for the general n can be expressed in a form of polynomial of degree $n+2$:

$$\sum_{i=0}^{n+2} D_i[S]^i = 0, \tag{21}$$

where the coefficients D_i's are given as follows:

$$D_i = \begin{cases} \beta_n^0, & \text{if } i=n+2 \\ \alpha_{n-1}^0 + \beta_{n-1} + \beta_n^0 B_t - \beta_n^0 S_t, & \text{if } i=n+1 \\ \sum_{j=0}^{n-i+1}\alpha_{i-2}^j + \sum_{j=0}^{n-i+2}\beta_{i-2}^j + \left(\sum_{j=0}^{n-i+1}\beta_{i-1}^j\right)B_t - & \\ \quad \left(\sum_{j=0}^{n-i}\alpha_{i-1}^j + \sum_{j=0}^{n-i+1}\beta_{i-1}^j\right)S_t, & \text{if } i=n,n-1,\ldots,2 \\ \alpha_{-1}^n + \left(\sum_{j=0}^{n}\beta_0^j\right)B_t - \left(1+\sum_{j=0}^{n-2}\alpha_0^j + \sum_{j=0}^{n}\beta_0^j\right)S_t, & \text{if } i=1 \\ -\alpha_{-1}^n S_t, & \text{if } i=0 \end{cases} \tag{22}$$

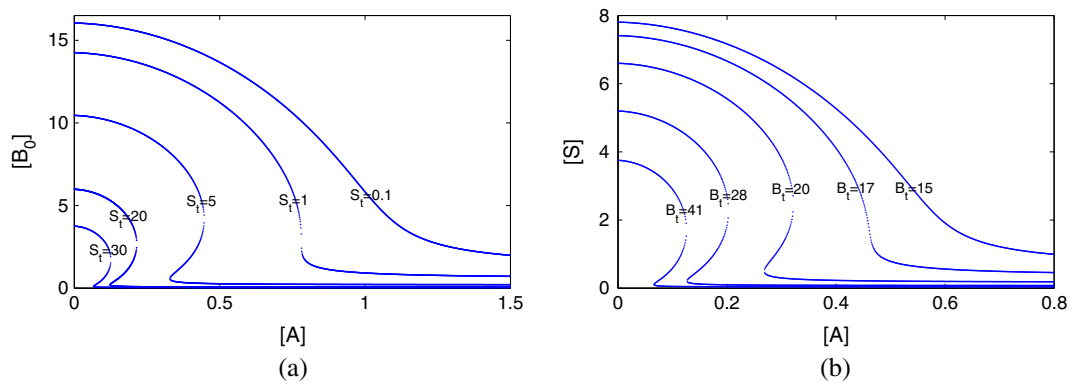

Figure 5. Simulation results with the kinase away from the scaffold and phosphatase on the scaffold for the case $n=2$. The parameters are selected identical for these two simulations as follows: $k_{\text{on}}^0 = 0.8, k_{\text{off}}^0 = 9.39, k_{\text{on}}^1 = 3.53, k_{\text{off}}^1 = 7.78, k_{\text{on}}^2 = 3.63, k_{\text{off}}^2 = 0.26, k_0 = 0.59, d_0 = 0.59, k_1 = 2.46$, and $d_1 = 0.027$. (a) Bistability takes place for a variance of total scaffold with a fixed amount of the total substrate 40; (b) bistability occurs for a variance of the total substrate when the total scaffold is fixed at 15.

Similar to the model when the kinase is co-localized on the scaffold as we discussed in the previous section, this system with $n = 1$ does not generate bistability, whereas it exhibits multistabilities for the case when $n > 1$. We have performed the same two computational explorations as previously discussed, and several similar observations can be made (See Figure 5). For instance, the bistability occurs only for a certain range of the total scaffold (with the total substrate fixed) and substrate (with the total scaffold unchanged). Interestingly, to allow for bistability, the ranges for both total scaffold and substrate are much narrower than the system with the kinase co-localized on the scaffold; that is, the model with the kinase away from the scaffold is not so robust to produce bistability as the model with the kinase on the scaffold. Moreover, for the system to have bistability, the ratio of binding and dissociate rates to the scaffold for the final phosphorylated form must be 20 times bigger than those for the other sites, which is opposite to the system when the kinase is co-localized on the scaffold.

3. Conclusion and discussion

In this paper, we have shown that a combination of multisite phosphorylation with scaffold binding can robustly produce bistability. To allow for bistability, we argue that phosphorylation and dephosphorylation must take place at different locations by using generic mathematical models. The system has only one steady state otherwise. In addition, we also find that the bistability tends to occur when the total substrate exceeds the total scaffold. One possible explanation for such observation is due to the competition for binding to free scaffolds between different forms of phosphorylation states. By treating parameters symbolically, we also thereby reduce the complexity of calculating steady states from simulating differential equations to finding the roots of polynomials, of which the degree depends on the number of phosphorylation sites N. For the ongoing work, we are extending the mathematical models discussed in this paper to further explore how ultrasensitivity or multistabilities will be affected by a random order of multisite phosphorylation without and with the presence of enzyme–substrate and phosphatase–substrate complexes.

Acknowledgements

This work was partially supported by NSF grant DMS1019544 and South Carolina EPSCOR GEAR grants.

References

1. Morrison D, Davis R. Regulation of MAP kinase signaling modules by scaffold proteins in mammals. *Annual Review of Cell and Developmental Biology* 2003; **19**:91–118.
2. Whitmarsh A, Davis R. Structural organization of MAP-kinase signaling modules by scaffold proteins in yeast and mammals. *Trends in Biochemical Sciences* 1998; **23**:481–485.
3. Wong W, Scott J. AKAP signalling complexes: focal points in space and time. *Nature Reviews Molecular Cell Biology* 2004; **5**:959–970.
4. Burack W, Cheng A, Shaw A. Scaffolds, adaptors and linkers of TCR signaling: theory and practice. *Current Opinion in Immunology* 2002; **14**(3):312–316.
5. Burack WR, Shaw AS. Signal transduction: hanging on a scaffold. *Current Opinion in Cell Biology* 2000; **12**:211–216.
6. Ferrell J, Cimprich K. Enforced proximity in the function of a famous scaffold. *Molecular Cell* 2003; **11**(2):289–291.
7. Flatauer L, Zadeh S, Bardwell L. Mitogen-activated protein kinases with distinct requirements for Ste5 scaffolding influence signaling specificity in Saccharomyces cerevisiae. *Molecular and Cellular Biology* 2005; **25**(5):1793–1803.
8. van Drogen F, Peter M. Spa2p functions as a scaffold-like protein to recruit the Mpk1p MAP kinase module to sites of polarized growth. *Current Biology* 2002; **12**(19):1698–1703.
9. Choi K, Satterberg B, Lyons D, Elion E. Ste5 tethers multiple protein kinases in the MAP kinase cascade required for mating in S. cerevisiae. *Cell* 1994; **78**(3):499–512.
10. Malleshaiah M, Shahrezaei V, Swain P, Michnick S. The scaffold protein ste5 directly controls a switch-like mating decision in yeast. *Nature* 2010; **465**(7294):101–105.
11. Pawson T, Scott JD. Signaling through scaffold, anchoring, and adaptor proteins. *Science* 1997; **278**:2075–2080.
12. Printen J. *et al.* Protein-protein interactions in the yeast pheromone response pathway: Ste5p interacts with all members of the MAP kinase cascade. *Genetics* 1994; **138**(3):609–619.
13. Barford D, Hu S, Johnson L. Structural mechanism for glycogen phosphorylase control by phosphorylation and AMP. *Journal of Molecular Biology* 1991; **218**(1):233–260.
14. Mann M, Ong S, Grønborg M, Steen H, Jensen O, Pandey A. Analysis of protein phosphorylation using mass spectrometry: deciphering the phosphoproteome. *TRENDS in Biotechnology* 2002; **20**(6):261–268.
15. Manning G, Whyte D, Martinez R, Hunter T, Sudarsanam S. The protein kinase complement of the human genome. *Science* 2002; **298**(5600):1912–1934.
16. Kholodenko B. Cell signalling dynamics in time and space. *Nature Reviews. Molecular Cell Biology* 2006; **7**(3):165–176.
17. Acuto O, Di Bartolo V, Michel F. Tailoring T-cell receptor signals by proximal negative feedback mechanisms. *Nature Reviews Immunology* 2008; **8**(9):699–712.
18. Schlessinger J. Cell signaling by receptor tyrosine kinases. *Cell* 2000; **103**(2):211–225.
19. Park K, Mohapatra D, Misonou H, Trimmer J. Graded regulation of the Kv2.1 potassium channel by variable phosphorylation. *Science* 2006; **313**(5789):976–979.
20. Huang C, Ferrell J. Ultrasensitivity in the mitogen-activated protein kinase cascade. *Proceedings of the National Academy of Sciences* 1996; **93**(19):10078–10083.
21. Markevich N, Hoek J, Kholodenko B. Signaling switches and bistability arising from multisite phosphorylation in protein kinase cascades. *Journal of Cell Biology* 2004; **164**(3):353–359.

22. Ingley E. Src family kinases: regulation of their activities, levels and identification of new pathways. *BBA-Proteins and Proteomics* 2008; **1784**(1):56–65.
23. Bardwell L, Liu X, Moore R, Nie Q. Spatially-localized scaffold proteins may simultaneously boost and suppress signaling. *PLoS Computational Biology* 2013. Submitted.
24. Salazar C, Hofer T. Multisite protein phosphorylation – from molecular mechanisms to kinetic models. *FEBS Journal* 2009; **276**(12):3177–3198.
25. Brown G, Hoek J, Kholodenko B. Why do protein kinase cascades have more than one level? *Trends in Biochemical Sciences* 1997; **22**(8):288–289.
26. Ferrell J. Tripping the switch fantastic: how a protein kinase cascade can convert graded inputs into switch-like outputs. *Trends in Biochemical Sciences* 1996; **21**(12):460–466.
27. Goldbeter A, Koshland D. An amplified sensitivity arising from covalent modification in biological systems. *Proceedings of the National Academy of Sciences* 1981; **78**(11):6840–6844.
28. Hooshangi S, Thiberge S, Weiss R. Ultrasensitivity and noise propagation in a synthetic transcriptional cascade. *Proceedings of the National Academy of Sciences* 2005; **102**(10):3581–3586.
29. Shacter-Noiman E, Chock P, Stadtman E. Protein phosphorylation as a regulatory device. *Philosophical Transactions of the Royal Society of London. Series B, Biological Sciences* 1983; **302**(1108):157–166.
30. Gunawardena J. Multisite protein phosphorylation makes a good threshold but can be a poor switch. *Proceedings of the National Academy of Sciences* 2005; **102**(41):14617–14622.
31. Serber Z, Ferrell J. Tuning bulk electrostatics to regulate protein function. *Cell* 2007; **128**(3):441–444.
32. Wang L, Sontag E. On the number of steady states in a multiple futile cycle. *Journal of mathematical biology* 2008; **57**(1):29–52.
33. Thomson M, Gunawardena J. Unlimited multistability in multisite phosphorylation systems. *Nature* 2009; **460**(7252):274–277.
34. Blenis J, Resh M. Subcellular localization specified by protein acylation and phosphorylation. *Current Opinion in Cell Biology* 1993; **5**(6):984–989.
35. Cyert M. Regulation of nuclear localization during signaling. *Journal of Biological Chemistry* 2001; **276**(24):20805–20808.
36. Ferrell J. How regulated protein translocation can produce switch-like responses. *Trends in Biochemical Sciences* 1998; **23**(12):461–465.
37. Karin M. Signal transduction from the cell surface to the nucleus through the phosphorylation of transcription factors. *Current Opinion in Cell Biology* 1994; **6**(3):415–424.
38. Pawson T. Specificity in signal transduction from phosphotyrosine-SH2 domain interactions to complex cellular systems. *Cell* 2004; **116**(2):191–203.
39. Van der Heide L, Hoekman M, Smidt M. The ins and outs of FoxO shuttling: mechanisms of FoxO translocation and transcriptional regulation. *Biochemical Journal* 2004; **380**(Pt 2):297–309.
40. Whitmarsh A, Davis R. Regulation of transcription factor function by phosphorylation. *Cellular and Molecular Life Sciences (CMLS)* 2000; **57**(8):1172–1183.
41. Liu X, Bardwell L, Nie Q. A combination of multisite phosphorylation and substrate sequestration produces switch-like responses. *Biophysical Journal* 2010; **98**:1396–1407.
42. Chan C, Liu X, Wang L, Bardwell L, Nie Q, Enciso G. Protein scaffolds can enhance the bistability of multisite phosphorylation systems. *PLoS Computational Biology* 2012; **8**(6):1–9.
43. Cateau H, Tanaka S. Kinetic analysis of multisite phosphorylation using analytic solutions to Michaelis–Menten equations. *Journal of Theoretical Biology* 2002; **217**(1):1–14.
44. Ciliberto A, Capuani F, Tyson J. Modeling networks of coupled enzymatic reactions using the total quasi-steady state approximation. *PLoS Computational Biology* 2007; **3**(3):e45.
45. Salazar C, Hofer T. Kinetic models of phosphorylation cycles: a systematic approach using the rapid-equilibrium approximation for protein–protein interactions. *Biosystems* 2006; **83**(2-3):195–206.
46. Salazar C, Hofer T. Versatile regulation of multisite protein phosphorylation by the order of phosphate processing and protein-protein interactions. *FEBS Journal* 2007; **274**(4):1046–1061.